Sample Canister Capture Mechanism for Mars Sample Return: Functional and environmental test of the elegant breadboard model ☆

R. Carta [a], D. Filippetto [a], M. Lavagna [b,*], F. Mailland [b,*], P. Falkner [c], J. Larranaga [d]

[a] *Politecnico di Milano, via La Masa 34, 20145 Milano, Italy*
[b] *OHB-CGS spa, via Gallarate 145, 20145 Milano, Italy*
[c] *European Space Agency (ESA), Keplerlaan 1, PO Box 299, NL-2200 AG Noordwijk, The Netherlands*
[d] *Aurora Technology B.V. for ESA, Keplerlaan 1, PO Box 299, NL-2200 AG Noordwijk, The Netherlands*

Received 31 December 2014
Received in revised form
8 June 2015
Accepted 5 July 2015
Available online 13 July 2015

1. Introduction

The Mars Sample Return (MSR) is an international endeavour mission to return samples from Mars surface to Earth. Several MSR mission architectures have been studied in the past years [1]; current approach (iMARS Phase 2) proposes to implement dedicated mission spacecraft elements spread in time over a sequence of launches: e.g. a Caching rover, a Mars orbiter including the Earth Return Vehicle and a Surface element, called Lander, including the Ascent Vehicle. In this architecture, the caching rover will be placed on Mars surface and a robotic system will collect samples of Martian rocks, soils and atmosphere. Once these samples have been collected, they will be loaded within an Orbiting Sample (OS) canister and the Ascent Vehicle will launch it from Martian surface into orbit.

☆ This paper was presented during the 65th IAC in Toronto.

* Corresponding authors.
E-mail addresses: riccardo.carta@mail.polimi.it (R. Carta), daniele.filippetto@polimi.it (D. Filippetto), lavagna@aero.polimi.it (M. Lavagna), FMailland@cgspace.it (F. Mailland), pfalkner@rssd.esa.int (P. Falkner), Jonan.Larranaga@esa.int (J. Larranaga).

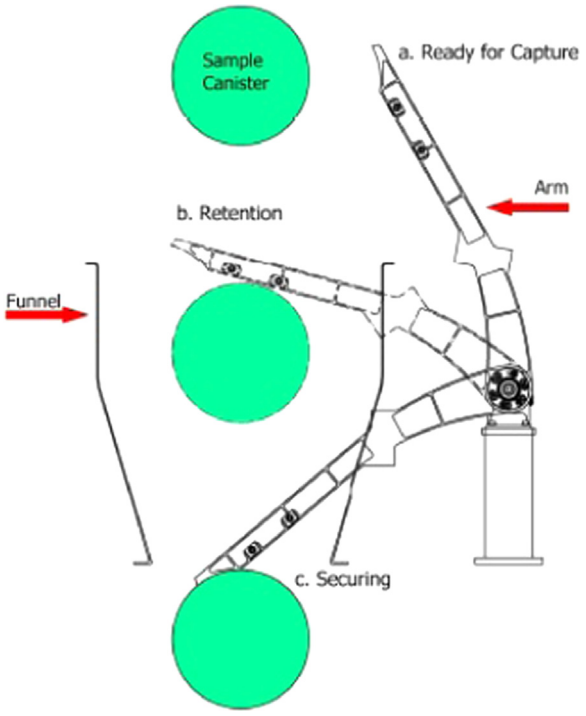

Fig. 1. SCCM operative modes.

After that, the orbiter waiting in Mars orbit will perform a rendezvous manoeuvre to capture the OS and secure it within the Earth re-entry capsule. Subsequently, the latter will return to Earth following a ballistic trajectory. In this context, the Sample Canister Capture Mechanism (SCCM) will be the robotic device aimed at ensnaring and securing the OS during the rendezvous manoeuvre; Fig. 1 shows the phases of the OS capture: starting from the Ready for capture configuration, once the OS enters the funnel, the arm starts closing to the retention configuration preventing the OS from escaping. The operation are concluded with the arm moving to the securing position thus driving the OS inside the Earth re-entry capsule.

Previous studies [2,3] investigated such a technology considering different concepts; this design activity, performed under the ESA Study "Sample Canister Capture Mechanism Design and Breadboard" [4], aimed at validating an alternative concept able to avoid the drawbacks of the previous solutions. The critical requirements driving the SCCM design are:

- OS mass of 6 kg;
- incoming velocity range of 5–15 cm/s;
- angular misalignment from nominal trajectory up to 5°;
- radial offset from nominal trajectory up to 10 cm;
- capture procedure completed in less than 90 s;
- SCCM resettable within 60 s from activation;
- maximum stowed envelop of 800 × 800 × 500 cm;
- lowest stowed natural frequency greater than 100 Hz;
- autonomous capture operation.

The present work takes place in the framework of an ESA contract primed by OHB-CGS and supported by Politecnico di Milano – Department of Aerospace Science and Technology aimed at:

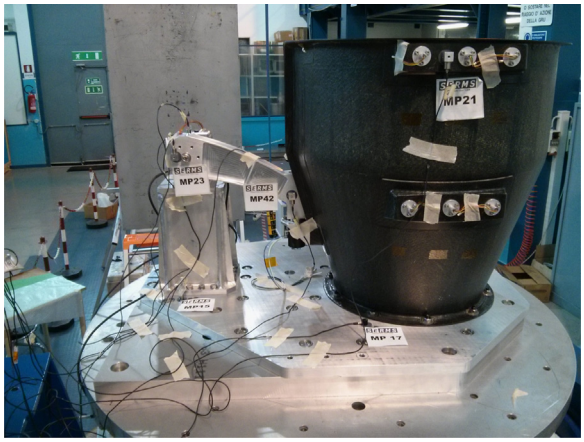

Fig. 2. Elegant Breadboard Model, as built.

- SCCM Elegant Breadboard Model MAIT;
- Ground functional tests;
- Environmental tests (thermal-vacuum and mechanical vibration tests);
- Flight test campaign on Parabolic Flight.

2. Breadboard manufacturing, assembly and integration

The Elegant Breadboard Model (EBM) was designed to be as representative as possible of the Flight Capture Mechanism (FCM) in order to guarantee the applicability of the tests results to the designed concept; in particular the EBM provides the key functionalities (e.g., arm operations) and performances (e.g., arm speed, operations duration) of the flight model. Components as the motor, the OS detection sensors (optical instruments) on the funnel and the Hold Down Release Mechanism (HDRM) selected for the EBM have the same functionalities of the FCM ones but were not space proven for procurement issues. The EBM was assembled and integrated at PoliMi-DAST, in particular the Funnel is made of CFRP, the Support Tower, the Arm and the Baseplate are Aluminium parts and the Actuation Chain is composed of Aluminium and Steel parts. The optical instruments were provided by CISAS together with their own electronics while the DC motor was purchased from Phytron GmbH. With respect to the previous EBM design [4] the motor changed, therefore some modifications were implemented to cope with the new mechanical test requirements; in particular the Support Tower and the Motor Interface Flange were extensively reshaped in order to improve the frequency response while reducing the acceleration levels of the Breadboard under qualification vibrational tests. These modifications, verified during the tests presented in this paper, shall be implemented on the Flight Capture Mechanism (Fig. 2).

Table 1
Breadboard measured vs. design mass budget [Kg].

Item	Design mass	As built mass
Arm assembly	1.69	1.76
Funnel assembly	5.09	5.92
Drive mechanism assembly	1.72	2.10
Tower assembly	0.95	2.58
Total	9.44	12.36

Table 1 summarizes the EBM main subsystems mass comparing the values estimated for the Flight Capture Mechanism concept design [4] with the measured masses of the manufactured breadboard. It is noticed that the higher mass of the Support Tower designed is due to the substantial reinforcement introduced to cope with the vibration frequency of the whole assembly.

3. Functional tests

The on-ground SCCM Test Campaign objective was raising the current Capture Mechanism technology to TRL 4 [5] and validating the developed SCCM design concept by means of limited environmental testing.

The Functional Tests (FTs) aimed at demonstrating functionalities and performances of the critical components of the EBM, as well as of the overall system. Such an objective was achieved performing the foreseen SCCM operations (arm release from stowed configuration, deployment, closure, reset and retention) and comparing the obtained results (in terms of arm speed, arm position, OS detection capability, etc.) to the defined requirements. In order to simulate the Mars Orbit 0-g environment, an ad-hoc test set-up was implemented, foreseeing the use of simulated 0-g Ground Support Equipment designed and assembled at PoliMi-DAST.

3.1. Objectives

The functional tests, performed on the assembled EBM, were divided into two main groups; the first one includes tests aimed at demonstrating key functionalities of some EBM components:

- *Arm actuation functionality*: a subset of the foreseen operations that the arm of the FCM would have to perform during its operative life were simulated in order to assess their correct execution.
- *HDRM functionality*: the release operation was executed in order to assess the functionality and effectiveness of the technical solution implemented.
- *Detection functionality*: the positioning of the OS detectors was verified by testing their capability to detect the presence of the arm and the OS during the SCCM operations.

The second group of tests aimed at characterizing the performances of some EBM components:

- Activation strategy validation, including the initial actuation phase up to 'retention complete'; for this validation a range of initial conditions was investigated.
- *Overall control strategy validation*: arm actuation speed for the different phases.
- Identification and assessment of possible critical geometries (i.e. relative positions between OS, funnel and arm).
- System robustness to single/multiple optical sensor failures.
- Measurement of Motorization Factors of the arm motor.
- Measurement of arm motor Maximum Torque.

Table 2
Arm operation tests.

Arm operations	Notes
Deployment	HDRM, no OS
Closure and reset	no OS
Retention	with OS

Table 3
OS initial conditions.

OS initial angle (°)	OS initial velocity (cm/s)	OS initial offset (cm)
0	5	0
5	10	10

Table 2 describes the operations tested for the demonstration of the arm actuation functionality.

The EBM performances tests gave important inputs for the following parabolic flight test campaign: in particular, the considered OS parameters with respect to the Funnel Body center were as follows: the OS initial angle, the OS initial velocity and the OS initial offset. For each of them, a set of different cases, reported in Table 3, was investigated. A scheme of the reported OS initial conditions with respect to Funnel position is shown in Fig. 3.

Considering the OS misalignment of 10 cm with respect to the Funnel center, four main positions, each one with an OS incident angle of 0° and 5°, were investigated:

- *Position* 0: OS aligned with respect to Funnel center.
- *Position* 1: OS misaligned of 10 cm with respect to Funnel center (OS position farther from the arm hinge).
- *Position* 2: OS misaligned of 10 cm with respect to Funnel center (OS position on the left wrt arm hinge. OS position on the right is symmetrical and then not tested).
- *Position* 3: OS misaligned of 10 cm with respect to Funnel center (OS position closer to the arm hinge).

As mentioned above, the system robustness to single/multiple detection sensors failure was assessed. In particular, a failure simulation was performed in order to verify the capability of the system of achieving its objective in such cases. In doing it, couples or multiple couples of sensors were assumed "damaged" thus not providing any support to the OS identification, this allowed testing if the EBM design is 1 failure/2 failures tolerant. It is remarked

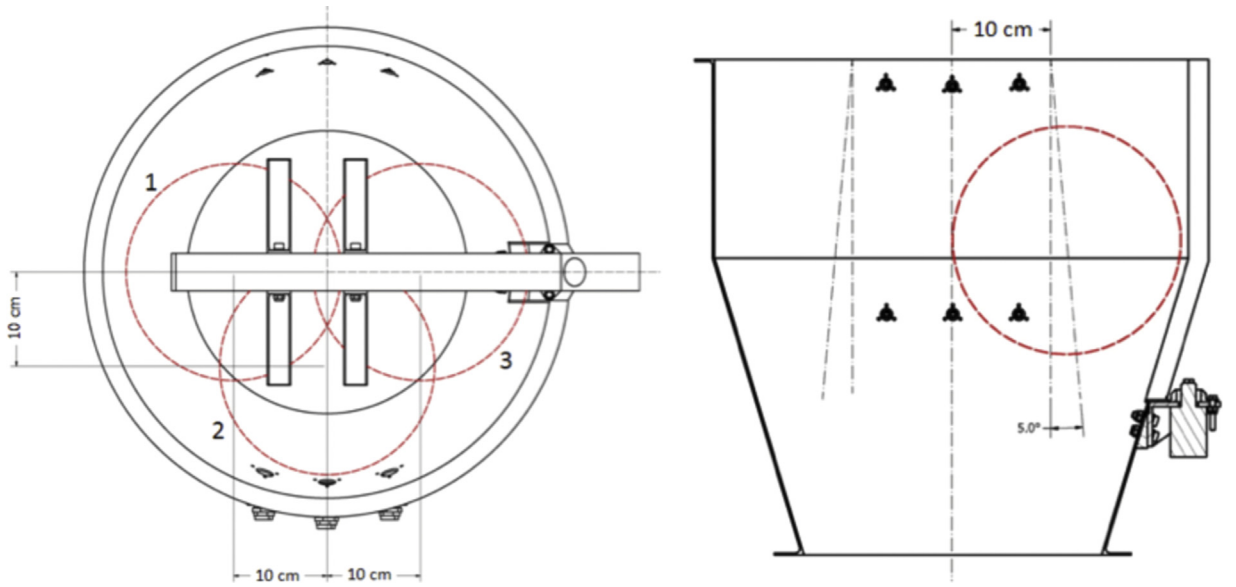

Fig. 3. OS contingency positions and angles.

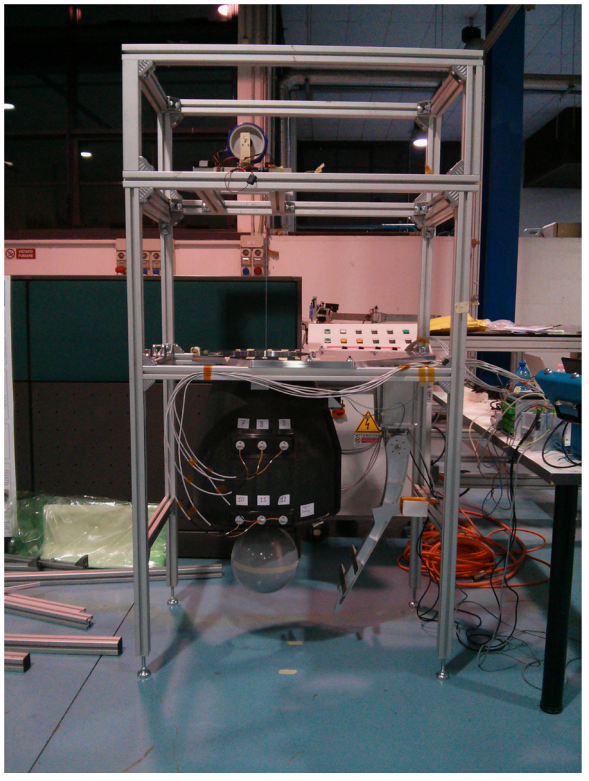

Fig. 4. 0-g Ground Support Equipment.

that the failure of a detection sensors was simulated both considering false positive triggering and failed detection.

3.2. Test set-up

For what concerns the execution of the FTs an ad-hoc facility was developed at PoliMi-DAST. The simulated 0-g Ground Support Equipment (GSE), shown in Fig. 4 consists of a dedicated truss structure, a Motor Assembly, a Motor Pulley, a Motor Support, an Encoded engine, a remote console to control the motor spooling speed dedicated to the simulation of different OS approaching speeds and an OS mock-up having the same size of the foreseen OS. This equipment allows also modifying the EBM position with respect to the OS in order to simulate different OS entrance conditions.

In order to perform the FTs, the EBM platform was accommodated on the truss structure, with its longitudinal axis placed in a vertical position with respect to the ground, and with the entrance of the funnel facing the floor. The OS mock-up was instead hanged to a thread and then raised up, at different speeds, by means of the Motor Pulley commanded by the remote console. The different relative positions of the OS with respect to the funnel entrance were obtained by moving the motor support with respect to the fixed position of the EBM on the truss structure. The “reversed” accommodation solution of the EBM was chosen in order to avoid possible interferences between the arm and the OS thread during the execution of the arm operations (e.g., retention). The GSE design allowed the EBM to be positioned also in a horizontal configuration in order to reduce the effects of the gravity on some of the measurements. This particular test configuration was used to measure the motor maximum torque and the motorization factors, minimizing the effect of gravity acting on the arm due to its own mass. A strain gauge half bridge was installed on the EBM motor shaft to measure the torque delivered by the motor while its internal temperature was monitored by means of the motor embedded temperature sensor. The gauge bridge set-up was calibrated before the test campaign. The OS speed was also calibrated, by means of a high-speed camera: the GSE motor angular rate was tuned to deliver the required OS vertical speed.

The main limitations of the GSE designed concern the effects of the gravitation forces on the relative dynamic and the impacts between the OS and the EBM; for this reason the estimation of this aspects was performed only during the parabolic flight experiment.

3.3. Results

The functional on-ground test campaign was overall successful demonstrating the effectiveness of the EBM design to achieve the required objectives, the motor and actuation chain performed as expected. Tables 4 and 5 summarize the FTs results.

The success of the functional test campaign allowed testing the EBM design in the environmental test campaign without design or configuration modifications.

4. Environmental tests

The environmental test campaign objective was demonstrating the EBM capability of withstanding the launch and thermal-vacuum environments. Such an objective was achieved by testing the EBM under relevant environmental conditions simulating the ones expected to be faced by the FCM during its mission [6]. The environmental test campaign occurred at Serms s.r.l., an Italian facility.

The Environmental Test campaign included the Thermal Vacuum Test (TVT), followed by a full set of functional tests in order to verify that no functional degradation had occurred on the EBM, and the Vibration Tests (VTs), followed by an additional set of functional tests to verify the EBM status.

4.1. Thermal vacuum tests

The TVT aimed at demonstrating the EBM capability to survive and operate at the thermal conditions foreseen for the FCM during its mission. The objective was to verify that the EBM mechanical parts (e.g., Arm Assembly and HDRM) were able to operate in the simulated thermal environment without performances degradation. The minimum and maximum testing temperatures for Arm Assembly and HDRM were selected taking into account the ones identified during the FCM design activity.

The test consisted in operating the EBM along a predefined temperature profile that foresaw a set of complete thermal cycles (1 cycle at non-operative conditions, 7 cycles at operative conditions) divided in a further set of steps having each one a dwell time of about 2 h to allow the thermal stabilization of the EBM components. Each step represents one of the four main temperature (mini-mum non-operative, minimum operative, maximum operative, maximum non-operative) derived from the thermal hot and cold worst cases identified during the FCM design activity and summarized in Table 6. A scheme of the complete TVT is shown in Fig. 5.

During the vacuum test, the pressure reached 10^{-6} bar before thermal regulation and remained stable below 10^{-5} bar for the entire duration of the test. The 8 thermal cycles were performed continuously acquiring temperature sen-sor data. The first cycle foresaw the simulation of the temperature profile associated with minimum and max-imum non-operative temperatures: during this cycle, the SCCM was not operated. The remaining 7 cycles simulated the temperature profile associated with the minimum and maximum operative temperatures: during each of these cycles, the arm movement was tested to verify its func-tionalities. Moreover, at the minimum temperature of the first of these cycles, the release of the HDRM was performed; it was not possible to repeat the HDRM release since the device was resettable only manually.

4.1.1. TVT set-up

The TVT foresaw accommodating the EBM inside a Thermal-Vacuum chamber in a horizontal configuration, as presented in Fig. 6. This configuration, required for the operations execution and the motor torque measurements during the thermal cycles, affected the duration of the thermal stabilization period: because of the experiment geometry in fact the EBM was not installed directly onto the chamber cold plate thus the main thermal exchange mechanism between EBM and chamber was radiation instead of conduction.

The acquisition system consisted in a set of thermocouples accurately distributed on the EBM structure. The sensor location on the EBM is described in Table 7 and Fig. 7.

4.1.2. TVT results

The TVT campaign successfully demonstrated the capability of the EBM to survive and operate in the foreseen thermal environment. Despite the high difference among the different EBM components in terms of thermal inertia the

Table 4
Functional tests results: functionalities.

Functionality tests	Results
Actuation arm functionality	Compliant
HDRM functionality	Compliant
Detection functionality	Compliant

Table 5
Functional tests results: performances.

Performance tests	Results
Arm closure/deployment duration	20 s
Motor maximum torque	11 Nm
Motorization factor	60
Failure mode	2 failure tolerant

Table 6
TVT temperatures.

Temperatures	Values (°)
Minimum non-operational/survival temperature	−25.0
Minimum operational temperature	−20.7
Maximum operational temperature	48.4
Maximum non-operational/survival temperature	62.2

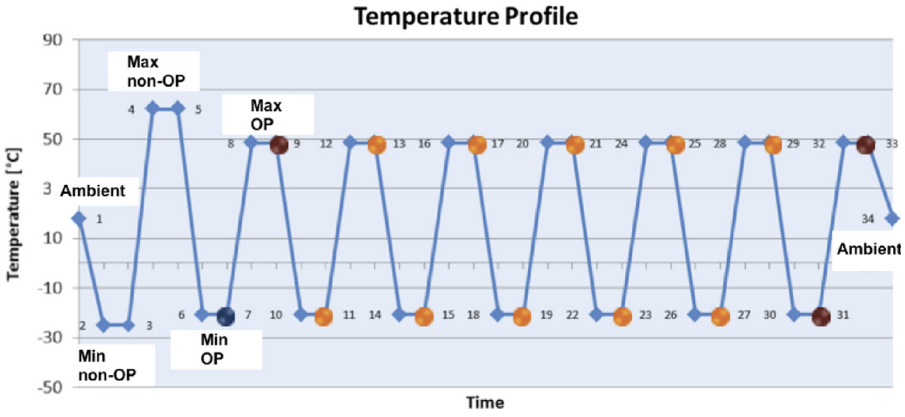

Fig. 5. TVT thermal cycles.

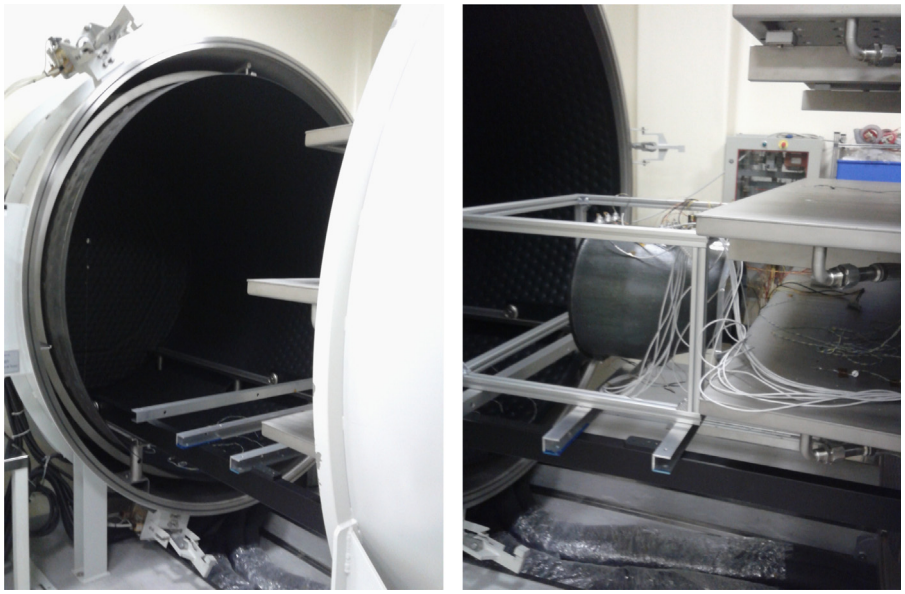

Fig. 6. TVT set-up.

Table 7
TVT temperature sensors location.

Temperature sensors ID	Location
A	Motor case (side)
B	Motor case (top)
C	Lug surface
D	Emitter
E	Receiver
F	HDRM
G	Arm tip
H	Arm shaft interface
I	Funnel top border
J	Funnel bottom (internal side)
K	Tower
L	Baseplate
M	Shaft/coupler

test campaign was executed as required from the test procedures. It is important to notice that the Funnel thermo-couples showed a temperature rate representative of the thermal-vacuum chamber temperature profile while the motor was slower to react to the temperature variations. In order to reduce the total duration of the test while applying the test procedure it was decided to set the chamber base plate and the shroud in the hot cases at 70 °C and 58 °C respectively for the non-operative and the operative cycles while in the cold cases the chamber temperature was always set at − 50 °C. This solution allowed reducing the ramps duration while being compliant with the stabilization requirements reported in the test procedure.

The details of the temperature profile of the motor and the Funnel are presented in Figs. 8 and 9 respectively. The motor temperature in the third hot operative case shows a spike: this anomaly, due to operators error, occurred after the execution of the foreseen functional test when the motor current was not set to 0 A as in the other cases. The error was identified and corrected and the motor tempera-ture never reached its operational limit; the tests performed in the following cycles did not highlight any malfunctioning of the hardware.

At the end of the TVT campaign the EBM functionalities were verified by performing a full functional test assessment.

4.2. Vibration tests

After the successful conclusion of the TVT the Vibration Tests (VTs) were performed. These tests aimed at verifying the EBM capability of withstanding the expected launch conditions. The VTs foresaw accommodating the EBM on a vibrating slip table for the tests along the funnel entrance plane (*X*- and *Y*-axes), and on the top of a shaker with a head expander for the tests along the longitudinal axis of the funnel (*Z*-axis). The shaker simulated the expected launch conditions for the FCM during the launch phase, while accommodated on top of the Orbiter and inside the launcher fairing. The VTs were performed with the arm in stowed configuration (the foreseen launch configuration) with the HDRM engaged. During the tests, accelerations in different points of the EBM were acquired in order to reconstruct its dynamic response to the vibration cycle. Moreover, after each vibration test, the integrity of the EBM structure was verified by visual inspection.

The functionalities of the EBM, at the end of the campaign, were further demonstrated by performing functional tests of the Arm Assembly (actuations with/without

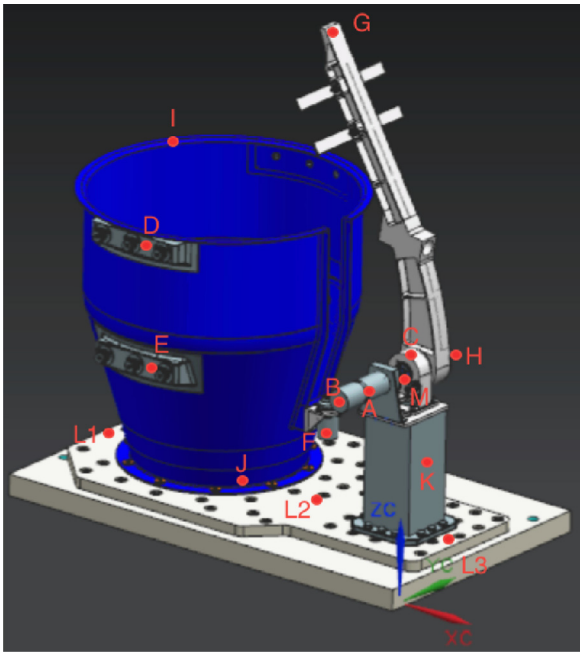

Fig. 7. TVT Temperature sensors position on the EBM.

Table 8
VT levels.

Test type	Description
Resonance search test	10–2000 Hz, 0.2 g
	5–21 Hz→ ±5.7 mm
Sine *X*-axis	21–60 Hz→10 g
	60–100 Hz→6 g
	5–21 Hz→ ±5.7 mm
Sine *Y*-axis	21–60 Hz→10 g
	60–100 Hz→6 g
	5–21 Hz→ ±5.7 mm
Sine *Z*-axis	21–60 Hz→20 g
	60–100 Hz→6 g
Random *X*-axis	9.03 gRMS
Random *Y*-axis	9.03 gRMS
Random *Z*-axis	14.00 gRMS

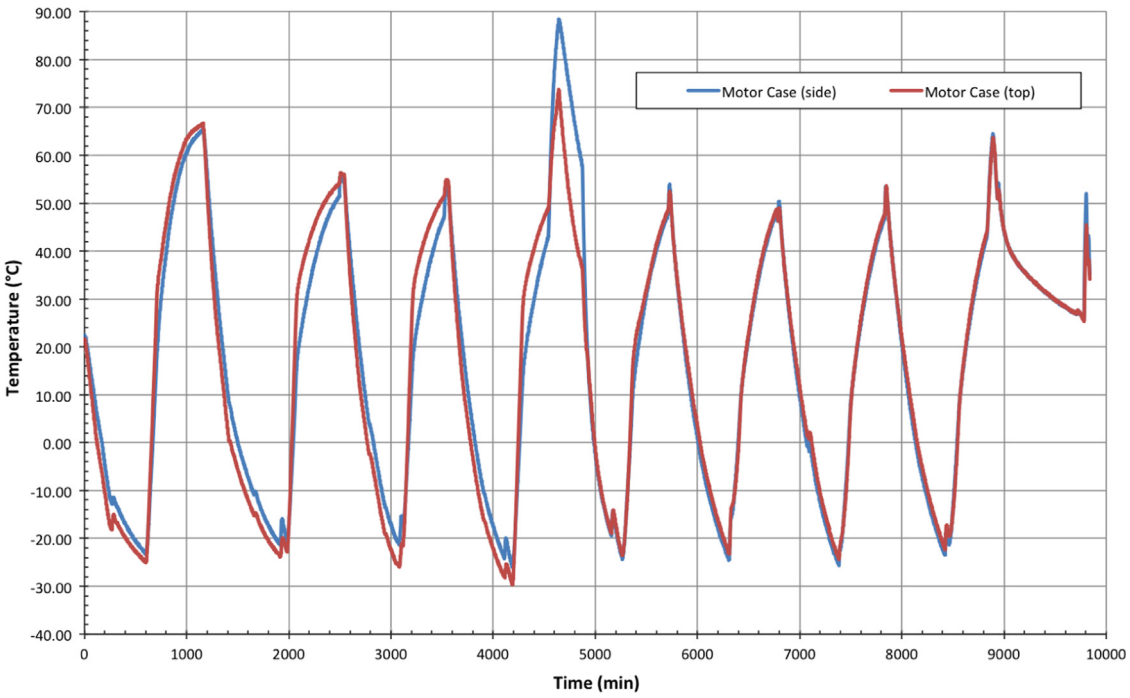

Fig. 8. TVT Motor temperature.

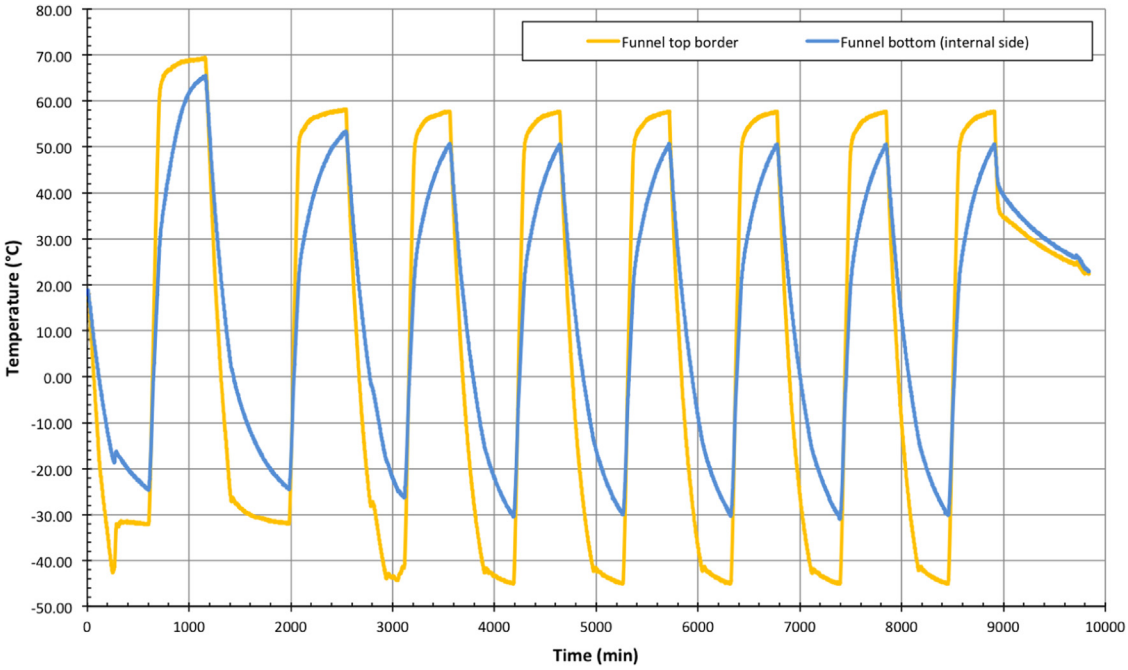

Fig. 9. TVT Funnel temperature.

load) and of the HDRM (release) in order to verify its structural integrity. More in detail, the Vibration Tests performed on each axis foresaw the following cases:

- Low level sine vibration test for resonance search;
- Sine vibration test with levels typical of a large launch system;
- Random vibration test with levels typical of a large launch system.

The levels applied were selected to be consistent with those of a typical large launch system (e.g., Ariane5) and are the same already used in a reference study case. It has to be pointed out that these are qualification levels, and were already considered during the design phase for the structural analysis of the FCM, (Table 8).

The sine vibration test along the *X* and *Y*-axes were executed at a lower level with respect to the *Z*-axis due to facility limitation: in fact the slip table was not able to provide 20 g acceleration to the EBM due to its high total mass. It is important to remark that this level reduction, agreed before the test execution, does not affect the validity of the test results: the sine spectrum foresaw applying 20 g below 60 Hz while the first natural frequency of the EBM is higher than 100 Hz causing the system to behave like a rigid body, thus responding at about 20 g. Moreover, from FEM analyses the random vibration response is higher than the aforementioned 20 g demonstrating alone the capability of the EBM to withstand the vibration loads.

4.2.1. Vibration tests set-up

The EBM was attached to the shaker and the slip table by means of a dedicated fixture designed to interface the EBM baseplate with the VTs facilities. Fig. 10 shows the EBM mounted on the facility support for testing. For the measurement of the EBM response to the solicitations a set of single-axis accelerometers was implemented: Table 9 and Fig. 11 show the measurement set-up for the VTs.

4.2.2. Vibration tests results

The VT campaign was overall successful, demonstrating the EBM capability of withstanding the input levels without degrading the system performances. The analyses of the results, in general satisfying, highlighted the need for an improved FE model for the correlation of the test results.

The frequencies of the first modes of the EBM are reported in Table 10. The columns represent the frequencies resulting from the FEM analysis, the resonance search before the VTs and the resonance search after the VT campaign. It is important to notice that in the FEM the constraint modelling increases the stiffness of the entire assembly. The percentage of reduction of the frequencies between the vibration test and the FEM analysis presented in Table 10 is always below 15%.

Fig. 12 shows the EBM response to the sine vibration test along the *Z*-axis, the graph displays the acceleration measured on the motor (CH65) and on the arm shaft (CH23). The sine test results highlighted the foreseen rigid behaviour of the EBM in the frequency range of these tests, which is lower than the breadboard first resonance frequency.

Table 11 summarizes the accelerations resulting from the random analyses on the FE model compared with the VTs results. The response along the *X*- and *Z*-axes is almost always lower than the predicted one while along the *Y*-axis some of the values measured are higher.

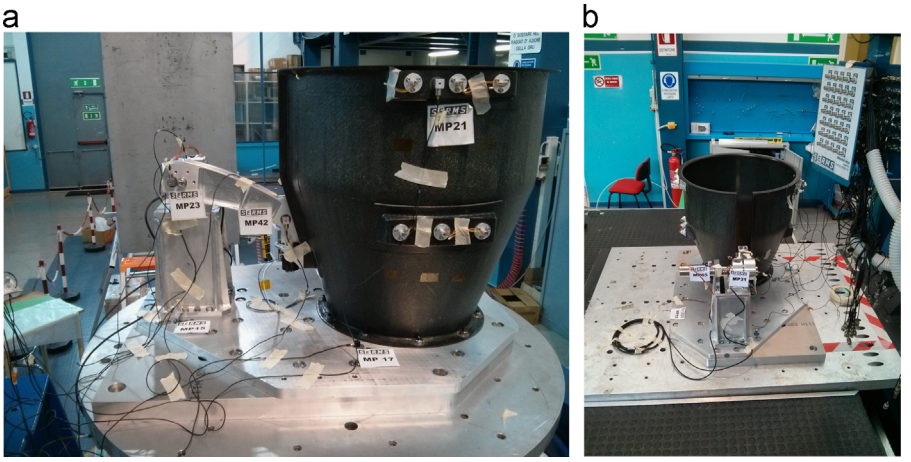

Fig. 10. VT set up (a) shaker and (b) slip table.

Table 9
Accelerometer locations.

Accelerometer sensors ID	Location
A	Baseplate (tower base)
B	Baseplate (funnel base)
C	Arm tip
D	Funnel top: outer optical barrier
E	Arm shaft
F	Lug top
G	HDRM/arm
H	Motor to tower flange

Table 10
Resonance search results.

Mode ID	FEM (Hz)	Before VT (Hz)	After VT (Hz)
1	123.75	107 (−13.5%)	107 (−13.5%)
2	134.24	117 (−12.8%)	117 (−12.8%)
3	141.56	125 (−11.7%)	125 (−11.7%)
4	150.17	138 (−8.1%)	136 (−9.4%)
5	151.22	145 (−4.1%)	144 (−4.8%)
6	223.21	200 (−10.4%)	201 (−10.0%)

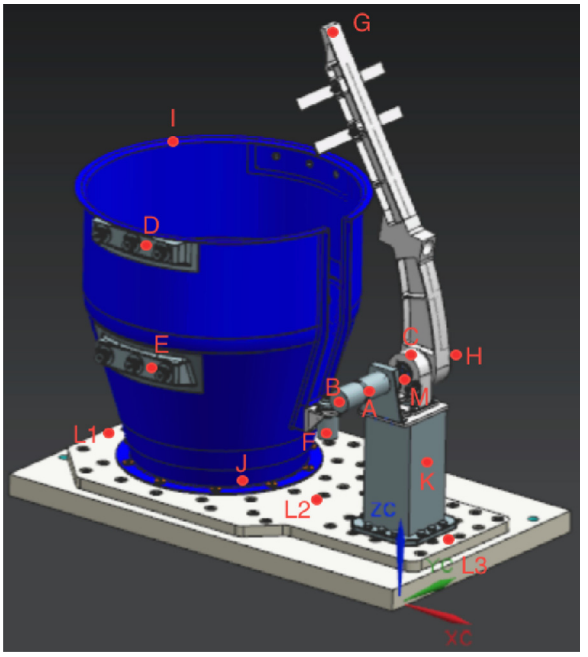

Fig. 11. VT accelerometer sensors position on the EBM.

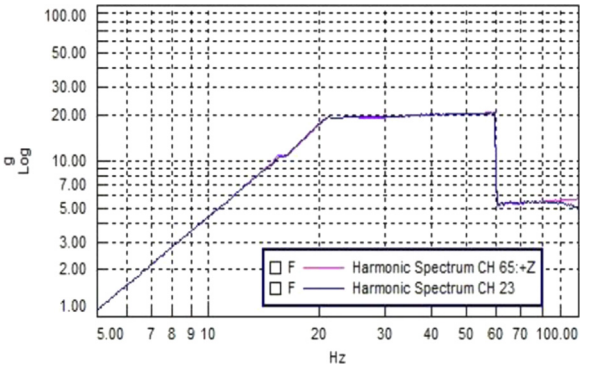

Fig. 12. Sine result, *Z*-axis: motor (ch: 65), arm shaft (ch: 23).

As mentioned above, it is important to notice that, in the FEM analysis, the constraints on the funnel were applied to the entire surface in contact with the baseplate in order to eliminate the presence in the results of a non-physical local mode between the screws connecting the funnel to the baseplate. This model simplification is bound to increase the stiffness of the connection thus increasing the frequencies of the modes.

At the end of the Vibration Test campaign the EBM functionalities were verified performing a full functional test assessment.

5. Parabolic flight experiment

The Parabolic Flight Test Campaign aimed at testing the EBM in representative 0-g conditions, raising the technology TRL to 6 (breadboard validation in relevant environment and

Table 11
Random vibration 3 response: *X*-axis.

Location	*X*		*Y*		*Z*	
	Test (g)	FEM (g)	Test (g)	FEM (g)	Test (g)	FEM (g)
Arm tip	85.87	68.75	104.79	165.88	131.48	134.32
Funnel top: outer optical barrier	58.11	59.27	116.04	97.33	81.33	46.23
Arm shaft	81.84	110.43	63.42	63.31	130.62	153.59
Lug top	64.89	107.29	115.20	75.32	57.54	70.77
HDRM/arm	72.87	106.26	64.44	81.89	95.58	100.24
Motor to tower flange	45.66	99.20	76.62	69.63	48.03	72.98

full scale) [5]. The Flight Test Campaign objective was demonstrating the EBM capability of performing the required capture operations in a relevant environment, here represented by the zero-g/microgravity conditions provided by the Parabolic Flight, which allowed testing the system with a realistic OS dynamics. In order to perform such a test, it would have been necessary having a free-floating experiment, as it was done in [7]; otherwise the atmospheric turbulence and aircraft pitch manoeuvres could have jeopardized the results. This was a critical issue for the test campaign since if, on one side, the free-floating solution allowed reducing the disturbances due to the atmosphere turbulence, on the other side, it raised safety issues for the crew that could have been hit by a sudden movement of the experiment structure, especially at the end of each microgravity phase. Moreover, it is important to notice that the results, in terms of impact forces between the OS and the SCCM, should have been carefully analysed since the exchanged momentum at the impact would be different with respect to the real one, because the test set-up structure (including the SCCM) is significantly lower in mass (about 40 kg) than the carrier of the Mars Sample Return mission (hundreds of kg).

A preliminary trade-off lead to consider a free-floating OS within a fixed rack comprising the EBM: this compromise helped both the estimation of the impact forces and reduced the safety risks having the EBM constrained to the aircraft with only the OS (about 6 kg) in free-floating condition. The cost of this compromise was the necessity to cope with the perturbation of the microgravity phases introduced by the aircraft itself.

The test took place during the 61st ESA Parabolic Flight Campaign at Novespace premises in Bordeaux-Merignac: it foresaw three days of tests and in each day 31 parabolas were performed. Each sequence of parabolas was divided into 6 sets of 5–6 parabolas.

5.1. Parabolic flight test plan

The Test Plan to be implemented for the Parabolic Flight Test Campaign was defined taking into account the specific environmental conditions simulated during the flight; furthermore, this plan was customized on parabolas set basis in order to test the higher number of parameters and conditions as possible.

In the first day of flight the tests were performed without taking into account OS misalignments and operating at fixed OS speed. This enabled verifying that all functionalities were correctly provided, calibrating the launcher and assessing the acceleration perturbation effects on the launcher performances. The results of these tests provided inputs for the selection of the launching strategy for the following days, in which the complete tests were performed. In particular, the tests foreseen for the first day were:

- Initialization (INIT), first set of 6 parabolas, used to verify the arm functioning, testing its opening, closure and holding at different angles (the OS was not used).
- Capture (CAPT), second set of 5 parabolas, used to verify the ability of the arm of maintaining the retention configuration with the OS already "captured" within the funnel.
- Transfer (TRA), third set of 5 parabolas, used to verify the "transfer" operation starting from the retention configuration with the OS inside the funnel. The first of the transfer tests was divided into two consecutive parabolas while in the following parabolas it was attempted to perform the test within one parabola.
- Launch (LNC), fourth and fifth sets of 5 parabolas, dedicated at verifying the OS launcher operations and the OS "real" trajectory. The OS was launched towards the funnel and its trajectory and movement were reconstructed by means of the selected instrumentation.
- Retention (RET), sixth set of 5 parabolas, aimed at verifying both OS launch and arm closure. The OS was launched and the triggering of the optical sensors activated the arm retention operation.

The following two test days were used to perform the complete test as presented in Fig. 13. Each complete test was divided into two parabolas using the first one for launch and retention operation and the second for transfer and securing. This plan allowed performing two complete tests each set of parabolas. The results of the first day, in particular of the transfer and the retention operations, were used to optimize the test sequence for the complete tests. Both in test days 2 and 3 the launch was performed considering different configuration of launcher offset and angle as foreseen in the system requirements (3); the OS initial conditions pattern was the same for both test days.

5.2. Parabolic flight test set-up

The EBM tested during the on-ground test campaign was modified in order to cope with the special conditions

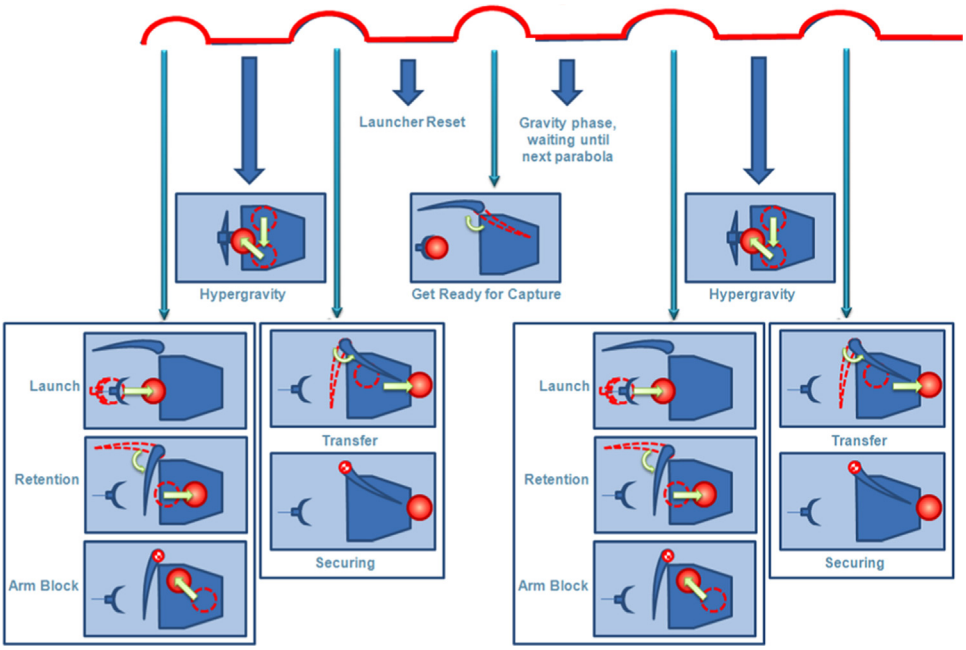

Fig. 13. Complete test schematics.

of a parabolic flight. In particular the free-floating OS was subjected up to 2 g of accelerations during the hyper-gravity phases at the beginning and at the end of each parabola: an impact of the OS onto the arm, in this condition, could generate a torque that the motor was not design to withstand. To solve this issue the EBM was modified in order to prevent the motor from working during hyper-gravity phases: the solution adopted was the use of a brake[1] mounted onto the arm shaft, which decoupled the motor from the arm during hyper-gravity phases thus blocking the arm.

Furthermore, it was necessary designing a device able to provide the OS with an initial trajectory and velocity suitable to test and verify the EBM capture capability: the OS launcher, shown in Fig. 14, was therefore designed with the following parameters as drivers:

- Initial OS velocity variable at least from 0.1 to 0.15 m/s;
- Easy 5° predefined attitude misalignment;
- Easy 10 cm predefined radial misalignment;
- OS retention under an acceleration of 2 g in all directions;
- Simple reset;
- Quick launch.

The actuation system is commanded by a manual release mechanism and the spring is responsible of providing the OS with the linear velocity required. The velocities required for the tests were selected by changing the initial compression of the spring in the actuation system while the orientation and misalignment of the OS trajectory was set moving the entire launcher structure with respect to the funnel.

A cylindrical container was also added at the bottom of the funnel to store the OS after the completion of the transfer tests.

The final design challenge was building a dedicated housing for the experiment compliant both with the test and the safety requirements for the parabolic flight. The Flight Experiment Rack (FER), as installed in the aircraft, is presented in Fig. 15 and it included:

- Capture Mechanism Breadboard modified for Parabolic Flight (arm brake, trap);
- OS Launcher;
- OS;
- Power Distribution System;
- DAQ and Control Unit.

It has to be remarked that the design of the rack, specifically the position of the launcher with respect to the funnel, was performed by analysing the results of simulations of the behaviour of the free-floating OS with respect to the funnel fixed to the aircraft. These simulations, however, considered the nominal 0-g condition and did not included the non-predictable perturbation accelerations.

5.3. *Parabolic flight test results*

The parabolic flight test campaign has proven successful in every aspect, allowing the validation of the design of the capture mechanism in microgravity environment. In particular the detection sensors triggered the arm closure in every tested condition and the actuation chain

[1] The selected device was the Mayr® electromagnetic safety brake ROBA-stop-M 16/891.100/28.

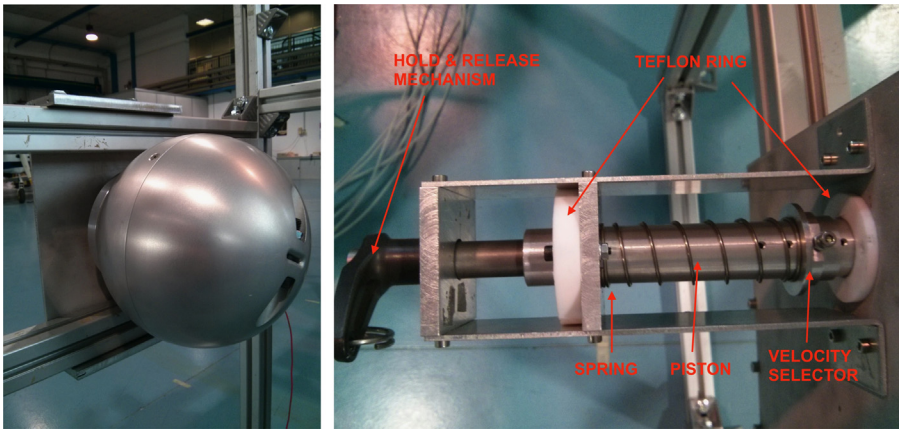

Fig. 14. OS launcher.

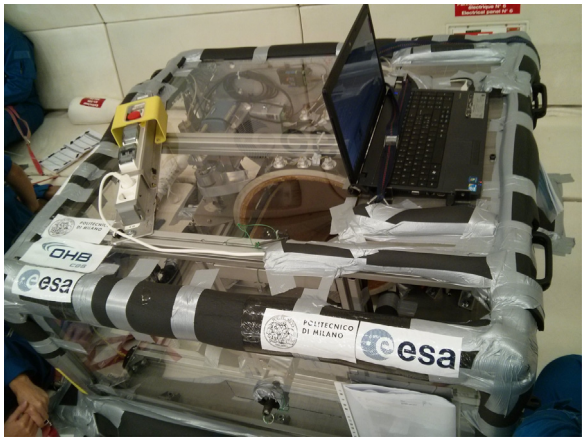

Fig. 15. Parabolic flight experiment installed.

demonstrated the EBM capability of capturing the OS once it entered the funnel and to transfer it into the trap withstanding also the impacts between OS and arm.

5.3.1. Test Day 1 results

Table A1 shows the results of the first day of test. Every test was completed successfully verifying the functionality of the components and the operations of the breadboard.

Is has to be remarked that for each INIT test only one operation of the arm (deployment or closure) was performed due to the limited microgravity period available. The results of the transfer tests established the possibility to perform this operation within one parabola without risk of pinching of the OS between arm and funnel walls. During the launch tests, even if the OS always entered the funnel and triggered the detection sensors, the high sensitivity of the OS launch to the aircraft perturbations during the microgravity phases was demonstrated by visual inspection of the test cases. This fact was highlighted also during the retention tests: twice the OS did not triggered the detection sensors after the launch. By visual inspection it was observed that the launcher performed its operations correctly but the aircraft perturbations heavily affected the OS trajectory. In these cases the OS was manually pushed inside the funnel by an operator, thus triggering the detection sensors and activating the retention operation, that was completed within the microgravity phase: these tests were still considered successful since the objective of the test was the retention operation and not the launch itself.

5.3.2. Test Day 2 results

Analysing the test results of the first day it was decided to update the test plan for the second and third days, (Table 12): since the operations duration were always much lower than the microgravity phases duration it was decided attempting to perform a complete test within one parabola instead of two avoiding stopping the operations for the hyper-gravity phases. The OS speed was measured and confirmed to be the expected 15 cm/s, it was thus decided to keep the OS speed for test day 2 and to increase it in test day 3 instead of testing the SCCM at lower speed (10 cm/s) because of the strong impact of the microgravity perturbations on the OS free floating dynamics after its release.

Table A2 presents the test results for the second day. The first two complete tests were executed in two consecutive parabolas (retention in the first and transfer in the second) as foreseen in the test procedure while in the other sets it was always attempted performing the complete test within one parabola: in some cases the perturbations caused the OS to trigger the detection sensors with a considerable delay after the launch proving impossible to complete the test within a single parabola; in these cases the test was stopped after the retention operation and the transfer was executed in the following parabola.

As already noticed in the first day, the perturbations strongly affected the test results: in fact, also in the failed tests, the launcher performed as expected but the OS, affected by the perturbations, did not entered the funnel thus not triggering the detection sensors.

In the test performed in the fourth parabola of the third set, after the launch and during the retention operation, the OS was exiting the funnel (due to perturbations effects) while the arm was closing causing pinching of the OS between arm and funnel border on the far side with respect to the hinge. In this case there was a loss of sync in the motor but the OS was

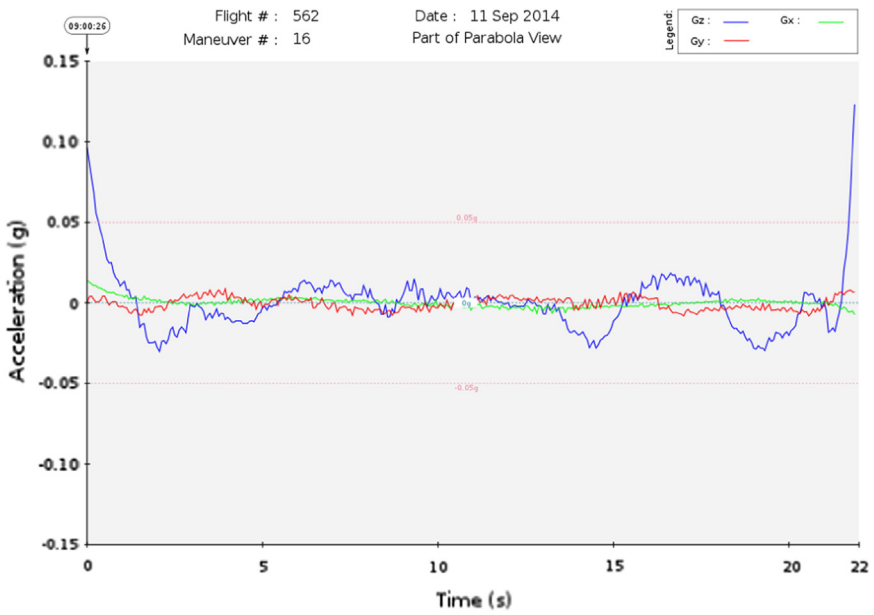

Fig. 16. 3rd day, 3rd set, 1st parabola aircraft accelerations.

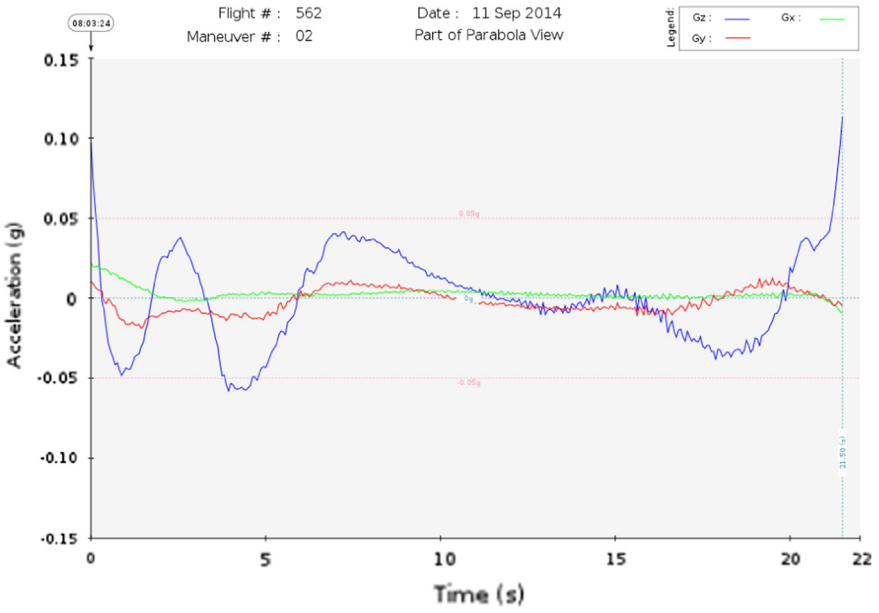

Fig. 17. 3rd day, 1st set, 3rd parabola aircraft accelerations.

still prevented from escaping and the transfer was completed: the test was therefore categorized as a success.

5.3.3. Test Day 3 results

The tests of the third flying day, whose results are presented in Table A3, were executed as in the second day with the difference the all the complete tests were per-formed within one parabola. As mentioned above, due to the effects of the perturbations on the OS trajectory, the OS launcher was set to a higher speed (20 cm/s) with respect to the previous day and to the 10 cm/s foreseen in the procedure. This condition was outside the design boundaries of the EBM (maximum OS incoming velocity of 15 cm/s) and caused higher impact forces than the one calculated in the design phase. Despite this changed configuration, the EBM completed the foreseen operations successfully proving the robustness and reliability of the design.

Even if the number of available test was limited due to the particular test environment, considering all the performed tests cases, an evaluation of the results summarized in Tables A2 and A3**?** lead to consider a percentage of success of 78% (14/18) during test day 2 and 71% (20/28) for test day 3. According to this and considering that the failed test were all

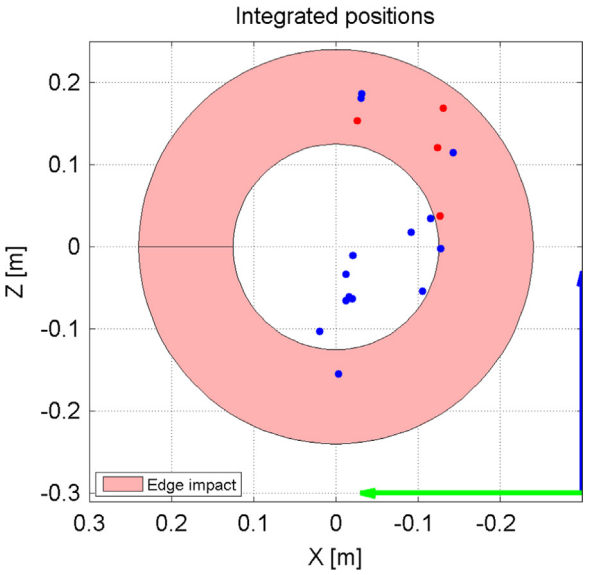

Fig. 18. 2nd day: integrated position.

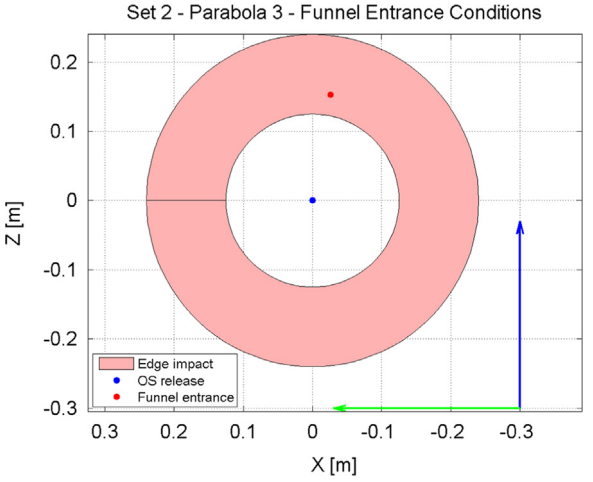

Fig. 19. 2nd day, 2nd set, 3rd parabola: OS estimated position at funnel entrance.

due to perturbation effects, it can be inferred that the OS speed does not have considerable effects on the capture test outcome; this result can be extend also to lower OS speeds (not tested due to perturbation effects), provided that the test is performed in a non-perturbed environment, since the time available for the EBM to complete the retention operation would be higher with a slower OS. On the other hand, a more detailed assessment of the test outcomes identified the worst-case initial condition to be the 3rd set test cases of both days, with 10 cm offset and 0° angle which shows the lowest percentage of success with 50% of failed capture tests.

5.3.4. *Microgravity perturbations*

Figs. 16 and 17 show two different aircraft acceleration profile during microgravity phases. These figures can be directly correlated to the results summarized in Table A3, which are a successful and failed test case respectively. Fig. 16 reports the acceleration pattern of a smooth parabola

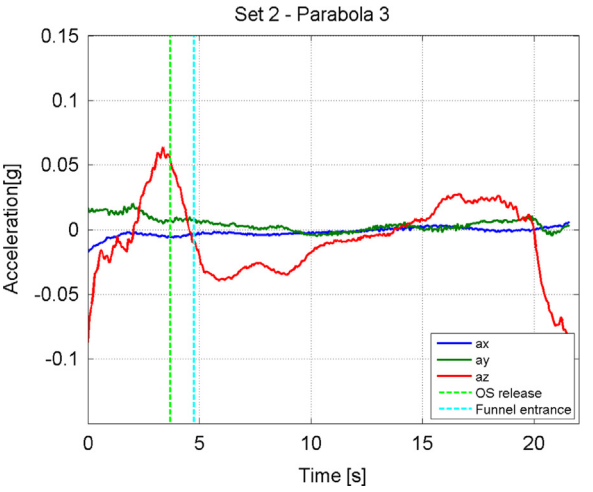

Fig. 20. 2nd day, 2nd set, 3rd parabola: microgravity phase accelerations. (For interpretation of the references to color in this figure caption, the reader is referred to the web version of this paper.)

while Fig. 17 is representative of a highly disturbed one. In particular it is remarked how, besides residual *Z* accelera-tion with a peak of about 0.05 g, relatively strong negative *Y* acceleration (the direction of the OS launch), of about 0.02 g, lasts for the first 5 s of microgravity. Considering the acceleration delivered by the OS launcher, lower than 0.04 g, this perturbation prevented the OS from reaching the funnel thus triggering the retention.

5.3.5. *Failed test*

In order to quantitatively assess the effects of the perturbations on the OS trajectory a detailed analysis of the aircraft acceleration after the OS launch and before the first impact with the funnel was performed; the release time with respect to the start of the microgravity was measured through the video data. From the launch instant the accelerations were integrated obtaining the velocity of the OS with respect to to the funnel; after adding the OS speed provided from the launcher a second integration step was executed to estimate the OS trajectory disturbed from the microgravity perturbations. Fig. 18 shows the center of the OS with respect to the funnel mouth at the entrance time: the blue and red dots represent respectively successful and failed tests while the red shaded area indicates when, due to the physical dimensions of the OS, an impact between the OS itself and the funnel edge occurred. It is remarked that all of the failed tests occurred when the OS impacted with the edge while entering the funnel and did not triggered the detection sensors. However, in some successful tests the OS impacted onto the funnel while entering and the SCCM was still able to complete the required operations. It is important to notice that the perturbations along *X* do not play a fundamental role in the OS entrance conditions while the vertical component is crucial in this aspect.

All the failed tests encountered were separately analysed to identify the causes of the unsuccessful result in each case. It is important to remind that the OS entrance position provided in this analysis is only an estimation based on the aircraft accelerations during the microgravity

phases. As an example, Fig. 19 shows the result of the test performed on 2nd day, 2nd set, 3rd parabola: the OS was launched with 0 cm offset and 0° angle and it impacted on the upped edge of the funnel thus not triggering the arm closure. The cause of this behaviour can be identified analysing the acceleration conditions when the OS was released, the vertical green line in Fig. 20: it is noticed that the launch occurred when a strong upward acceleration was present in the aircraft causing the OS to impact on the upper edge of the funnel thus a failed test.

6. Lesson learnt and conclusion

6.1. Lesson learnt

The test campaign performed on the SCCM was overall successful however some possible improvements were highlighted during the activity both from a design and a MAIT point of view. In particular some components selected for the EBM, such as the open/close arm sensors, mechanical microswitches, were damaged during the functional tests repetitions therefore a more robust component is suggested to be used during further test of the design. Moreover, the assembly operation was difficult for some component, as the HDRM and the interface between arm and support tower; an updated design for this component is therefore needed.

Table 12
Test days 2 and 3 OS initial conditions.

Set ID	OS initial angle (°)	OS initial offset (cm)
1	0	0
2	0	0
3	0	10
4	5	0
5	5	10
6	5	10

Regarding the functional tests execution no problems were encountered while for the environmental tests it is recommended to select a different facility able to cope in every test case proposed with the high mass of the EBM for the vibration tests and to accommodate the EBM in a configuration able to improve the thermal exchange mechanism during the thermal vacuum test.

6.2. Conclusion

The functional test campaign was successfully completed: the EBM performances were evaluated during the functional tests at PoliMi-DAST facility; the breadboard design proved effective both at system and component level in laboratory environment.

The environmental test campaign was also successfully completed, demonstrating the EBM ability of withstanding the mechanical and thermal loads induced during all mission phases. Moreover the breadboard performances were not affected from these environmental loads.

These results raised the SCCM concept TRL to 4.

The parabolic flight test campaign was successfully performed demonstrating the EBM full functionality in relevant 0-g environment. The expected number of test cases were almost doubled since the arm actuation proved able to execute a complete test within a single parabola: these enabled extracting a more meaningful statistic of successful/failed tests. No major remarks needs to be reported on the hardware itself, the major issue to cope with was the strong perturbation experienced by the OS during the free-floating phase within the experiment rack. The failed tests were due to the perturbations rather than EMB malfunctioning; in particular the early seconds of microgravity are crucial for the positive outcome of the test case since the OS was released by hand at the very beginning of the parabola, thus the OS launch was very sensitive to the microgravity quality, which was completely random and unpredictable.

Table 13
Parabolic flight test results summary.

Test day	Test case	Speed (cm/s)	Offset (cm)	Angle (°)	Success over launches (%)	Success with triggered sensors (%)	Success with OS inside the funnel for more than 4 s (%)
1	INIT	–	–	–	100	100	100
	CAPT	–	–	–	100	100	100
	TRA	–	–	–	100	100	100
	LNC	15	0	0	100	100	100
	RET	15	0	0	100*	100*	100*
2		15	0	0	83 (5/6)	100 (5/5)	100 (5/5)
		15	10	0	50 (2/4)	100 (2/2)	100 (2/2)
	C-15	15	0	5	100 (4/4)	100 (4/4)	100 (4/4)
		15	10	5	75 (3/4)	100 (3/3)	100 (3/3)
	TOT	–	–	–	78 (14/18)	100 (14/14)	100 (14/14)
3		20	0	0	80 (8/10)	80 (8/10)	100 (8/8)
		20	10	0	50 (2/4)	50 (2/4)	100 (2/2)
	C-20	15	0	5	60 (3/5)	75 (3/4)	100 (3/3)
		20	10	5	78 (7/9)	100 (7/7)	100 (7/7)
	TOT	–	–	–	71 (20/28)	83 (20/24)	100(20/20)

Some of the tests performed under low perturbations conditions demonstrated the possibility of the OS to enter directly into the trap after triggering the detection sensors without the help of the arm. On the other hand, when the OS impacted onto the funnel walls, it started to rotate along the walls in a plane parallel to the funnel entrance. It is important to notice that is not possible to establish if this behaviour was in any way helped by the acceleration perturbations. From this point of view an improvement for the parabolic flight experiment could be the implementation of an automatic release mechanism triggered by an acceleration sensor: this solution could avoid failed launches due to perturbation.

Parabolic flight test environment poses strong limitation for the testing of low speed free-floating objects in a fixed envelope. The environment is dominated by a random unpredictable gravity noise: a microgravity background level of 0.05 g prevent maintaining a foreseen free-floating trajectory with respect to a fixed target. Higher speed mitigates this effect by reducing the free-floating time span.

Table 13 summarizes the results of the tests performed during the parabolic flight campaign. In particular, for the complete tests three success percentages are reported:

- "Success [%] over launches" is the number of successful tests for each initial condition over the total number of launches performed during the flights. This percentage is useful to identify the critical initial conditions in this particularly perturbed environment;
- "Success [%] with sensors triggered" is the number of successful tests over the number of times the OS triggered the sensors after the launch. This percentage is still affected by the perturbation, as described in the analysis above;
- "Success [%] with OS inside funnel for more than 4 s" is the number of successful test cases over the number of tests in which the OS did not exit the funnel before 4 s, after triggering the sensors. Remembering that the retention operation duration was set at 7 s, the 100% success rate demonstrates the robustness of the EBM performances not only inside the design parameter, but also in non-nominal conditions for offset, angle, speed and retention duration.

The objective of the test campaign to raise the TRL to 6 was fully achieved.

Acknowledgements

The authors would like to thank PoliMi-DAST technical team for the support in manufacturing of the EBM and logistics; Mayr Italia for the kind procurement of the brake; ESA Human Spaceflight Department in particular Mr. Vladimir Pletzer for the support in parabolic flight experiment preparation and schedule; Novespace, in particular Mr Frederic Gai for the support in the experiment rack design and in-flight procedure definition; last but not least, ESA MREP team for supporting the decision of PoliMi being part of the OHB-CGS team to implement the MREP SCCM technology activity.

Table A1
Parabolic flight first day test results.

Test ID	Result	Remarks
1.1	N/A	Not available for test
1.2	Success	Only deployment
1.3	Success	Only closure
1.4	Success	Only deployment
1.5	Success	Only closure
1.6	Success	Only deployment
2.1	Success	
2.2	Success	
2.3	Success	
2.4	Success	
2.5	Success	
3.1	Success	First half transfer
3.2	Success	Transfer completion
3.3	Success	
3.4	Success	
3.5	Success	
4.1	Success	
4.2	Success	
4.3	Success	
4.4	Success	
4.5	Success	
5.1	Success	10 cm offset
5.2	Success	10 cm offset
5.3	Success	
5.4	Success	
5.5	Success	
6.1	Success	No arm/OS impact
6.2	Success	Arm/OS impact
6.3	Fail	10 cm offset
6.4	Fail	10 cm offset
6.5	Success	10 cm offset, arm/OS impact

Table A2
Parabolic flight second day test results.

Test ID	Result	Remarks
1.1	N/A	Not available for test
1.2	Success	
1.3	Success	Arm/OS impact
1.4	Success	
1.5	Success	Arm/OS impact
1.6	Success	
2.1	Success	Arm/OS impact
2.2	Success	Transfer
2.3	Fail	
2.4	Success	Arm/OS impact
2.5	Success	
3.1	Fail	
3.2	Success	Switch to retention, Arm/OS impact
3.3	Success	Transfer
3.4	Success	Arm/OS pinching
3.5	Fail	
4.1	Success	
4.2	Success	
4.3	Success	
4.4	Fail	
4.5	Success	
5.1	Fail	
5.2	Success	Switch to retention
5.3	Success	Transfer
5.4	Success	Switch to retention, Arm/OS impact
5.5	Success	Arm/OS impact

Table A3
Parabolic flight first day test results.

Test ID	Result	Remarks
1.1	N/A	Not available for test
1.2	Success	
1.3	Fail	Arm/OS impact
1.4	Success	
1.5	Success	
1.6	Success	Arm/OS impact
2.1	Success	
2.2	Success	
2.3	Success	
2.4	Success	Arm/OS impact
2.5	Fail	
3.1	Success	0 offset, Arm/OS impact
3.2	Success	Arm/OS impact
3.3	Fail	
3.4	Success	Arm/OS impact
3.5	Fail	
4.1	Success	
4.2	Fail	
4.3	Fail	
4.4	Success	
4.5	Success	Arm/OS impact
5.1	Success	
5.2	Fail	
5.3	Success	
5.4	Fail	
5.5	Success	Arm/OS impact
6.1	Success	
6.2	Success	
6.3	Success	Arm/OS impact
6.4	Success	Arm/OS impact
6.5	N/A	

Appendix A. Test Day 1, 2 and 3 results

See Tables A1–A3.

References

[1] The iMARS Working Group Preliminary Planning for an International Mars Sample Return Mission, 2008, Available at: http://mepag.jpl.nasa.gov/reports/iMARS_FinalReport.pdf.

[2] ACDM Aurora – Capture/Docking Mechanisms, Summary Report, ACDM-SEN-SR-010, 16, March 2007, ESA Contract 18185/04.

[3] Capture/Docking Mechanism Testing (CDMT) Inflatable Capture Mechanism (ICM), ESA Contract 20006/06/NL/EK.

[4] F. Mailland, K. Geleen, P. Coste, Zaccariotto, E. Monchieri, Sample Canister Capture Mechanism for Mars Sample Return: Design and testing of an Elegant Breadboard Model, 63rd International Astronautical Congress, Naples, Italy 2012.

[5] ECSS-E-AS-11C Definition of the TRLs and their Criteria of Assessment, ECSS Secretariat, ESA-ESTEC, Requirements and Standards Division, Noordwijk, The Netherlands, October 2014, Available at: ecss.nl.

[6] ECSS-E-ST-10-03C Testing, ECSS Secretariat, ESA-ESTEC, Require-ments Standards Division, Noordwijk, The Netherlands, June 2012, Available at: ecss.nl.

[7] R. Kornfeld, J. Parrish, S. Sell, Mars Sample Return: testing the last meter of rendezvous and sample capture, J. Spacecr. Rock. 44 (May–June (3)) ;44(2007), http://dx.doi.org/10.2514/1.2609.